JOURNAL OF COMPUTATIONAL PHYSICS 89, 187–206 (1990)

A Numerical Method for Finding the Ground States of One-Dimensional Systems

KEVIN HOOD*

Centre de Recherche en Physique du Solide et Département de Physique, Université de Sherbrooke, Sherbrooke, Québec, Canada J1K 2R1

Received September 19, 1988; revised July 24, 1989

Griffiths and Chou introduced a method of effective potentials for finding the ground states of a class of systems that can be described by classical one-dimensional Hamiltonians with nearest neighbor interactions. In practice the effective potentials must be solved numerically by discretization on a grid of N points. Existing algorithms have calculation times that vary as N^2 or worse. We show how this can be reduced to linear in N by means of straightforward optimizations that take advantage of the properties of the effective potentials. © 1990 Academic Press, Inc.

1. INTRODUCTION

Consider the problem of finding the ground states of a one-dimensional chain of atoms with Hamiltonian of the form

$$\mathscr{H} = \sum_n [V(u_n) + W(u_{n+1} - u_n)], \tag{1}$$

where u_n is the position of the nth atom, $V(x)$ is a periodic substrate potential, and $W(x)$ is an interaction potential acting between adjacent atoms. A common approach is to consider the force equilibrium equations

$$\frac{\partial \mathscr{H}}{\partial u_n} = V'(u_n) + W'(u_n - u_{n-1}) - W'(u_{n+1} - u_n) = 0, \tag{2}$$

where primes indicate spatial derivatives. Unfortunately (2) is satisfied, not only for ground states, but for any extremal configurations including those that maximize (1). Nonetheless, when $W(x)$ is everywhere convex ($W''(x) > 0$), (2) can be written as a two-dimensional area preserving map and the trajectories of this map contain information on the ground states of (1) [4]. When $W(x)$ is not an everywhere

* Present address: Xerox Research Centre of Canada, 2660 Speakman Drive, Mississauga, Ontario, Canada L5K 2L1.

0021-9991/90 $3.00

convex function of x the map is no longer well defined and cannot be used as easily if at all.

Recently, Griffiths and Chou [1, 2] introduced the method of *effective potentials* by means of which one can find the exact ground state of (1) even when $W(x)$ is a *nonconvex* function, that is when $W''(x) < 0$ for one or more values of x.

In this paper, we present a modified version of the numerical iterative method that was described in Refs. [1, 2]. To the unmodified version, whose execution time varies roughly as N^2, where N is the size of the grid on which the effective potential is discretized, we add a number of optimizations that result in an execution time that is roughly linear in N. The rest of the paper is organized as follows: In Section 2 we describe the method of effective potentials and the discretization that is used to obtain numerical results. We then show, in the same section, how three types of optimization on the basic numerical procedure are implemented. In Section 3 we present numerical results including an analysis of the errors present in our numerical method and results for the method's performance for different levels of optimization. Finally, in Section 4, we conclude with some comments on how one might extend our numerical procedure to solve for the effective potential in more complicated situations such as when second neighbor interactions are added to (1).

It should be made clear from the outset that the numerical procedure presented here is based on a number of assumptions for which we have no analytic proof. Our justification for them is twofold: First, the method works; when the optimizations are removed the same results are obtained albeit at the expense of increased execution time. Second, it is found that our assumptions are valid for a number of characteristic cases and it is hoped that the same behavior will occur whenever similar conditions are present.

2. The Method of Effective Potentials

The method of effective potentials that was introduced by Griffiths and Chou [1, 2] involves solving the nonlinear eigenvalue equation

$$R(u_{n+1}) + \lambda = V(u_{n+1}) + \min_{u_n} [W(u_{n+1} - u_n) + R(u_n)]$$
$$= \mathscr{K} R(u_n). \tag{3}$$

The *eigenvector*, $R(u_n)$, will be referred to as the *right* effective potential and physically corresponds to the minimum energy of a semi-infinite chain of atoms; $\{u_i\}: i \in [-\infty, n]$; when the rightmost atom is held fixed at the position u_n. The *eigenvalue*, λ, corresponds to the average energy per atom in an infinite chain and $\mathscr{K}$ is a functional operator which has the effect of adding one more atom to the chain. Similarly, for a semi-infinite chain of atoms; $\{u_i\}: i \in [n, \infty]$; when the

leftmost atom is held fixed at the position u_n, one can define the *left* effective potential

$$S(u_{n-1}) + \lambda = V(u_{n-1}) + \min_{u_n} [W(u_n - u_{n-1}) + S(u_n)]$$

$$= \mathscr{K} S(u_n). \tag{4}$$

The full effective potential felt by an atom in an infinite chain of atoms is then

$$F(u) = R(u) + S(u) - V(u). \tag{5}$$

The derivation of (3)–(5) is detailed in Ref. [2]. Note that R, S, and F all have the same periodicitiy as V. In this work we are only interested in systems with inversion symmetry, $V(u) = V(-u)$, in which case $S(u) = R(-u)$ and we need only concentrate on the calculation of $R(u)$ which, henceforth, we shall refer to simply as the effective potential. Once $R(u)$ has been calculated, it is a simple matter to find the ground state positions of the atoms. Define the map [1, 2]

$$\tau(u_{n+1}) = u_n \tag{6}$$

to be that u_n which minimizes the right-hand side of (3) for a given u_{n+1}. Physically, if a semi-infinite chain has its rightmost atom fixed at u_n then the sequence $u_{n-1} = \tau(u_n)$, $u_{n-2} = \tau(\tau(u_n))$, $u_{n-3} = \tau(\tau(\tau(u_n)))$,..., gives the ground state atomic positions for atoms successively farther to the left in the chain. As $\tau(x)$ is iterated it converges to the ground state map (far from the rightmost atom, the effects of this atom on the chain are exponentially small and the atomic positions will tend toward those of the infinite chain). For a commensurate ground state, $\tau(x)$ converges to a limit cycle with finite period. For incommensurate ground states $\tau(x)$ does not repeat.

A. *The Discretized Effective Potentials*

An analytic solution to (3) is, in general, impossible and it is usual to solve for the *discretized effective potential* on a grid of N evenly spaced points. As a result of the discretization, one cannot distinguish between atoms whose ground state positions correspond to distances closer than about one grid spacing and so, for finite N, one will never find incommensurate or higher order commensurate ground states. Nevertheless, it is often the case that low order commensurate configurations account for most of the volume in large regions of parameter space, and in these regions the discretized numerical method is appropriate and often gives clues as to how higher order commensurate (and perhaps incommensurate) states occur in the phase diagram.

The discretization need only be done over one full period of $R(u)$ which, as mentioned, has the same periodicity as $V(u)$. In some cases only a fraction of a full period need actually be considered. Let the discretized approximation to $R(u)$ be

$R_N(u)$ for a grid of N points where u is understood to be taken on this grid. We require that $R_N(u)$ satisfy (3) with the minimization now occurring over the discrete set of points. Given a point v on a chosen grid of N points, it will not generally be the case that $R_N(v) = R(v)$ and hence the discretization leads to there being an *intrinsic error* in the calculation of the effective potential. An important question is then: under what circumstances is the intrinsic error negligible and to what extent is $R_N(u)$ a good approximation to $R(u)$. For instance, does $R_N(u)$ lead to the correct ground state periodicity. One method of measuring how well $R_N(u)$ approximates $R(u)$ is to consider how $R_N(u)$ converges as N is increased by successive *grid doublings*. This is the approach that we use and that will be discussed in more detail in Sections 2B and 3B. It should be mentioned that the problem of solving the discrete form of (3) falls into a class of problems occurring in minimax algebra [5]. To solve for the discrete form of (3) we use a variation of the iterative method originally used by Griffiths and Chou [1, 2] in which $R_N(u)$ is solved iteratively:

$$R_N^{(k+1)}(u) = \frac{1}{m+1}\left[\mathscr{K}_N R_N^{(k)}(u) + m R_N^{(k)}(u)\right] - C_{k+1}, \tag{7}$$

where $R_N^{(k)}$ is the kth approximation to R_N, C_{k+1} is a constant chosen so that the minimum value of $R_N^{(k+1)}(u)$ is zero, and $\mathscr{K}_N$ represents the operator $\mathscr{K}$ on the discrete grid. A second approach—a modified Karp–von Golitschek method—has recently been described by Florida and Griffiths [3]. In our method, convergence to a reasonable effective potential always seems to occur though we have no proof that this should be so. The constant m in (7) is chosen for optimum convergence of $R_N^{(k)}$ to $R_N \equiv R_N^{(\infty)}$. A measure of this convergence is given by

$$\Delta_N^{(k)} = \max_u |R_N^{(k)}(u) - R_N^{(k-1)}(u)| \tag{8}$$

and $R_N^{(k)}$ is considered to have converged when

$$\Delta_N^{(k)} < \varepsilon(N), \tag{9}$$

where $\varepsilon(N)$ is a measure of the required precision and is usually taken to be some small fraction of the characteristic energy scale as determined by $V(x)$. Since $\Delta_N^{(k)}$ does not always converge monotonically we generally require that (9) be satisfied for several consecutive iterations of (7). A more quantitative analysis of these points is presented in Section 3A. The error in the calculation of $R_N(u)$, resulting from terminating the iteration of (7) at a finite value of k, will be referred to as the *iteration error* (we assume that $R_N^{(k)}(u)$ does converge to $R_N(u)$ as $k \to \infty$). We have tried different values of m in (7) and find $m \approx 1$ ($m = 1$ was used in Ref. [1, 2]), to be optimal with convergence always found to occur. For $m \gg 1$, $\Delta_N^{(k)}$ always seems to converge albeit slowly since $R_N^{(k)}(u)$ is heavily weighted by $R_N^{(k-1)}(u)$. For $m \ll 1$, on the other hand, (7) does not seem to converge at all. Henceforth we only consider $m = 1$ though some interesting results when $m = 0$ are reported briefly in Section 3C.

In (7), each iteration requires solving for $R_N^{(k)}(u)$ at N different values of u. At each u, one must solve for $\mathscr{K}_N R_N^{(k)}(u')$ which involves a minimization over βN values of u', where β is a model dependent constant (typically $1 \lesssim \beta \lesssim 2$). The calculation time for R_N is given by

$$t_{ex} = \beta t_p \mathscr{I}(N, \varepsilon)\, N^2, \tag{10}$$

where t_p is the calculation time per point (u, u') and $\mathscr{I}(N, \varepsilon)$ is the number of iterations required for convergence and depends on both N and $\varepsilon = \varepsilon(N)$. Note that $\mathscr{I}(N, \varepsilon)$ also depends on the exact form of the potentials being considered. In most cases the dependence on N is found, numerically, to be weak so that (10) depends predominantly on the square of N. Note also that $\mathscr{I}(N, \varepsilon)$ depends on the initial guess $R_N^{(0)}$. It is rarely possible to obtain a good guess for $R_N^{(0)}$ and we generally choose $V(x)$ as a starting point. With the optimizations that are described below the initial guess turns our to be unimportant. In addition, because of the discretization of $R(u)$, the map (6) must also be discretized:

$$\tau(u) \to \tau_N(u).$$

When $\tau_N(u)$ is iterated it must converge to a limit cycle of period N or less and hence only commensurate states are seen.

B. *Grid Doubling*

One way to obtain $R_N^{(0)}$ is by means of successive doublings of the number of points on the grid. Starting with N_0 grid points, with N/N_0 a power of 2, $R_{N_0}^{(\mathscr{I}_0)}$ can be quickly calculated to within a precision ε_0, where we use the simplified notation $\varepsilon_d = \varepsilon(N_d)$ and $\mathscr{I}_d = \mathscr{I}(N_d, \varepsilon_d)$. It is then easy to to obtain $R_{N_1}^{(0)}$ from $R_{N_0}^{(\mathscr{I}_0)}$ by interpolation, where $N_1 = 2N_0$. More generally, $R_{N_{d+1}}^{(0)}$ is obtained from $R_{N_d}^{(\mathscr{I}_d)}$, where $N_d = N_0 2^d$ and d refers to the number of grid doublings that have been performed. With D total grid doublings, the solution time is given by

$$t_{ex} = \beta t_p \left(\frac{N}{2^D}\right)^2 \sum_{d=0}^{D} 4^d \mathscr{I}(N/2^{D-d}, \varepsilon_d). \tag{11}$$

Numerically it is found that the number of iterations is roughly independent of N for a given ε_d. Setting $\mathscr{I}(N/2^{D-d}, \varepsilon_d) = \mathscr{I}_0$ for $d < D$ then, as $D \to \infty$

$$t_{ex} \approx \beta t_p N^2 [\tfrac{1}{3}\mathscr{I}_0 + \mathscr{I}_D] \tag{12}$$

which shows that the total calculation time is dominated by that of the final largest grid.

As has already been mentioned, if v is a point on a grid of both N_d and $N_{d+1} = 2N_d$ points then there is an intrinsic error and it is generally not true that $R_{N_{d+1}}(v) = R_{N_d}(v) = R(v)$, since both $R_{N_{d+1}}(v)$ and $R_{N_d}(v)$ are only discrete

approximations to the true effective potential $R(v)$. A quantitative measure of the intrinsic error is, within the grid doubling scheme, given by

$$\Delta R_N^{\text{rms}} = \left[\frac{1}{N}\sum_n^{N_d} [R_N(u_n) - R_{2N}(u_n)]^2\right]^{1/2},$$

$$\Delta R_N^{\max} = \max_n |R_N(u_n) - R_{2N}(u_n)|.$$

ΔR_N^{rms} describes, as a function of N, the overall convergence of $R_N(u)$ to the undiscretized $R(u)$ while $\Delta R_N^{\max}$ measures the worst case convergence indicating how uniformly R_N converges. As is shown in Section 3A, both ΔR_N^{rms} and $\Delta R_N^{\max}$ show a power law behavior in N and can be used to estimate the maximum intrinsic error in $R_N(u)$.

It is worth commenting on the two types of error, intrinsic and iteration. For a chosen grid of N points and as (7) is iterated there is, after the kth iteration, a total error that is a combination of the intrinsic and iteration errors in $R_N^{(k)}(u)$. As $k \to \infty$ the iteration error generally decreases to zero while the intrinsic error, which depends on the chosen discretization, remains fixed. Given N, it is not worth reducing the iteration error too much since once the iteration error is smaller than the intrinsic error, the precision gain in iterating (7) becomes negligible. A more quantitative analysis of this point is given in Section 3A.

C. *Range Restriction*

In this section we describe a second optimization which we refer to as *range restriction*. It is convenient to rewrite (3) as follows:

$$\begin{aligned} R(u_{n+1}) + \lambda &= V(u_{n+1}) + \min_{u_n} G(u_{n+1}, u_n), \\ G(u', u) &= W(u' - u) + R(u). \end{aligned} \tag{13}$$

The discretized version of (7) using (13) is (with $m = 1$) given by

$$R_N^{(k+1)}(u') = \tfrac{1}{2}[V(u') + \min_u G_N^{(k)}(u', u) + R_N^{(k)}(u')] - C_{k+1}, \tag{14}$$

where it is understood that u and u' are taken from the set of N grid points. The discretized notation for $G_N^{(k)}$ is the same as for $R_N^{(k)}$ defined in Section 2A. Consider the difference

$$\begin{aligned} \delta_N^{(k)}(u) &= G_N^{(k)}(u', u) - G_N^{(k-1)}(u', u) \\ &= R_N^{(k)}(u) - R_N^{(k-1)}(u) \end{aligned} \tag{15}$$

which, as a function of k, describes how $G_N^{(k)}(u', u)$ converges to $G_N \equiv G_N^{(\infty)}(u', u)$. Assume that this convergence is bounded by the exponential

$$|\delta_N^{(k)}(u)| \leqslant \delta_N(u)\, e^{-\alpha(u)k} \tag{16}$$

for any given u. Assuming (16) to be valid, then an upper bound for the amount that $G_N^{(k)}(u', u)$ can change in going to from $k = l$ to $k = \infty$ is given by

$$|\Delta G_N^{(l)}(u', u)|_{\max} \leqslant \sum_{k=l+1}^{\infty} |\delta_N^{(k)}(u)| = \frac{|\delta_N^{(u)}(u)|}{e^{\alpha(u)} - 1}. \tag{17}$$

$|\Delta G_N^{(l)}(u', u)|_{\max}$ is an upper bound for the deviation of $G_N^{(k=l)}(u', u)$ from its value when $k \to \infty$. Numerically it is frequently found that $\delta_N^{(k)}(u)$ behaves as an exponentially decaying oscillating function of k so that the actual deviation is smaller than the maximum value given by (17). If, for a given u', $G_N^{(l)}(u', v) > G_N^{(l)}(u', w) + |\Delta G_N^{(l)}(u', v)|_{\max} + |\Delta G_N^{(l)}(u', w)|_{\max}$ then the point v will never minimize $G_N(u', u)$ and therefore in (14) one need only consider the set $\mathscr{S}_N^{(k)}(u')$ of u such that

$$G_N^{(k)}(u', u) - \frac{2\delta_N(u)\, e^{-\alpha(u)k}}{e^{\alpha(u)} - 1} < G_N^{(k)}(u', u_0^{(k)}(u')), \tag{18}$$

where $u_0^{(k)}(u')$ is the u at which $G_N^{(k)}(u', u)$ is minimized. Those u for which (18) is not satisfied can never minimize $G_N^{(k)}(u', u)$ whenever (16) holds. In this way, for each value of u', we restrict the range of u that need be considered and, as $k \to \infty$, $\mathscr{S}_N^{(k)}(u')$ will contain only the single element, $u_0^{(k)}(u')$.

In practice one does not know the exponents $\alpha(u)$ and it is not convenient to keep track of $\mathscr{S}_N^{(k)}(u')$ for which N^2 storage elements are required. Therefore we implement the above range restriction in a numerically convenient way: From (8) and (15) one has that

$$\Delta_N^{(k)} = \max_u |\delta_N^{(k)}|$$

so that, if (16) holds, then $\Delta_N^{(k)}$ converges exponentially with exponent $\alpha = \max_u \alpha(u)$. Then (18) can be written

$$G_N^{(k)}(u', u) - g\Delta_N^{(k)} < G_N^{(k)}(u', u_0^{(k)}(u')), \tag{19}$$

$$g \cong \frac{2}{e^{\alpha(u)} - 1}. \tag{20}$$

g is a constant which is determined numerically (see Section 3A).

We replace the set $\mathscr{S}_N^{(k)}(u')$ by two bounds which bracket all of the elements of $\mathscr{S}_N^{(k)}(u')$. The minimization in (14) is performed only for those u that are between the left bound $\mathscr{L}_N^{(k)}(u')$ and the right bound $\mathscr{R}_N^{(k)}(u')$. Initially the bounds are chosen sufficiently large so as to bracket all u that might minimize $G_N(u', u)$:

$$\mathscr{L}_N^{(0)}(u') = \mathscr{L}_N^{\min}(u'); \qquad \mathscr{R}_N^{(0)}(u') = \mathscr{R}_N^{\max}(u'). \tag{21}$$

After each iteration k, and for each u', $\mathscr{L}_N^{(k)}(u')$ is increased until (19) is not

satisfied. $\mathscr{R}_N^{(k)}(u')$ is decreased in a similar manner. This is done until $\mathscr{L}_N^{(k)}(u') = \mathscr{R}_N^{(k)}(u') = u_0^{(k)}(u')$, at which point the minimum of $G_N^{(k)}(u', u)$ is fixed at $u_0^{(k)}(u')$.

As an example of the choice of $\mathscr{L}_N^{\min}(u')$ and $\mathscr{R}_N^{\max}(u')$, assume that it is known, from some analysis of the potentials V and W, that only bond lengths satisfying $a < z_n < b$ are possible for all n, where $z_n = u_{n+1} - u_n$. For instance, physical constraints often require that $u_n < u_{n+1}$ so that $a \geqslant 0$. Also, when $R(u)$ is periodic in u with period l, and $W(z)$ is a monotonically increasing function of z for $z > z'$, for some z', then it is not hard to show from (3) that $b < z' + l$. Given a and b then one chooses

$$\mathscr{L}_N^{\min}(u') = u' + a \tag{22}$$

$$\mathscr{R}_N^{\max}(u') = u' + b. \tag{23}$$

It is understood that the positions in (22), (23) are taken on a regular grid with a spacing between grid points of l/N. In this particular example one finds $\beta = (b-a)/l \lesssim z'/l + 1$, where β was defined in the paragraph above (10).

Two examples of $G(u', u)$ are shown schematically in Fig. 1. In Fig. 1a, the most common case, the solid line represents $G(u', u)$ for some value of u' and as a function of u. The broken line shows schematically how the numerical approximation $G_N(u', u)$ behaves. Although $G(u', u)$ and $G_N(u', u)$ do not coincide, for both functions the minimum is near u_0 and the secondary minimum at u_1 is higher that u_0 by more than the intrinsic error of $G_N(u', u)$ so that as convergence is approached only the minimum at u_0 is bracketed. A second case can occur at particular values of u' as shown in Fig. 1b. $G(u', u)$ has two minima, at u_0 and u_1 with $G(u', u_0) < G(u', u_1)$, that are degenerate to within the intrinsic error of $G_N(u', u)$. As a result, it can occur that $G_N(u', u_1) < G_N(u', u_0)$ as shown by the broken line. During much of the convergence both of the nearly degenerate minima, at u_0 and u_1, are bracketed along with the points between them where (19) is not satisfied. At some value $k = K$, as $G_N^{(k)}(u', u)$ converges, it will happen that

$$G_N^{(K)}(u', u_0) - G_N^{(K)}(u', u_1) > \varepsilon \Delta_N^{(K)}$$

and subsequently, for $k \geqslant K$, only the minimum at u_1 will be bracketed. Since u_1 does not correspond to the correct minimum of the undiscretized $G(u', u)$ then the resulting effective potential will not agree with that obtained without range restriction though the ground states for the two cases may or may not correspond. The importance of this intrinsic error effect is discussed in the next section.

D. *Range Restriction with Grid Doubling*

Including grid doubling with range restriction proceeds as described in Section 2B except that now the bounds $\mathscr{L}_N^{(k)}(u')$ and $\mathscr{R}_N^{(k)}(u')$ must be rescaled after each doubling. The safest way to do this is to reset $\mathscr{L}_{2N}^{(0)}(u')$ and $\mathscr{R}_{2N}^{(0)}(u')$ to the minimum and maximum values given in (21) after each grid doubling. This results, however, in a calculation time that varies as N^2. If $R_N(u)$ is a good approximation

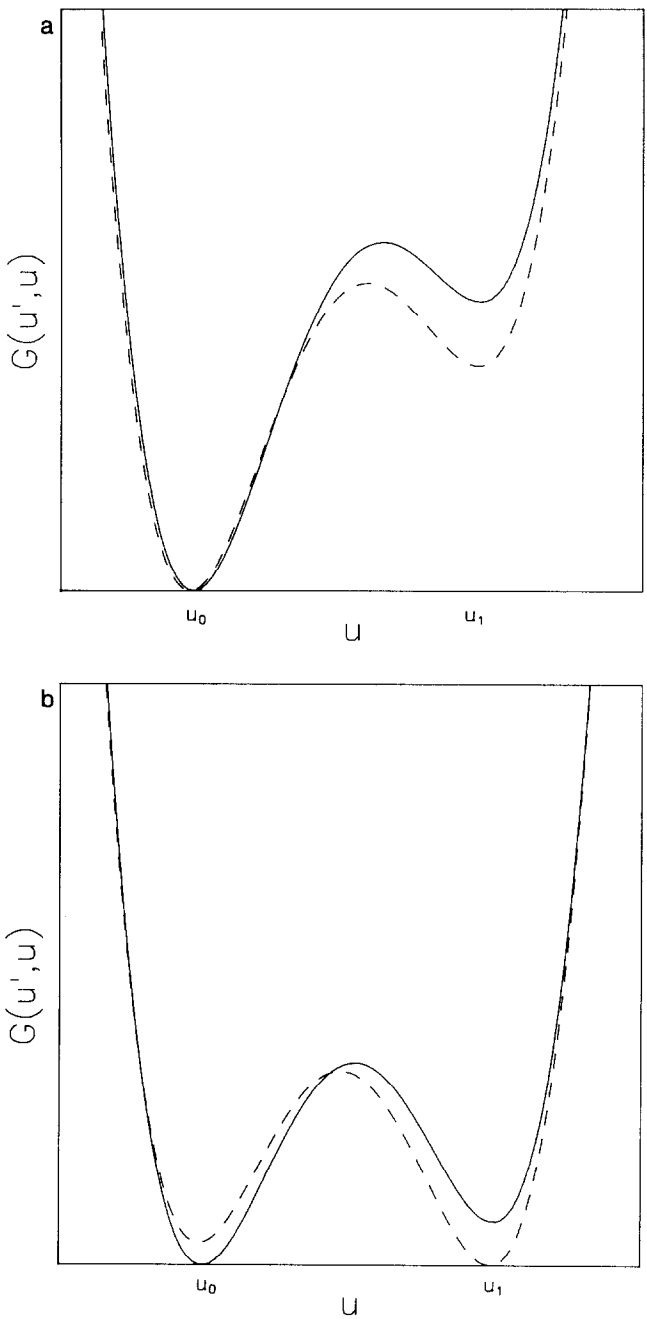

FIG. 1. Two schematic examples of $G(u', u)$ (solid line) and its discrete approximation $G_N(u', u)$ (dashed line) as a function of u for fixed u'. (a) Only one minimum occurs within the intrinsic error of $G(u', u)$. (b) A secondary minimum occurs within the intrinsic error of the correct minimum.

to $R_{2N}(u)$, then $\mathscr{L}_N^{(k)}(u')$ and $\mathscr{R}_N^{(k)}(u')$ can be scaled in a way that leads to a linear dependence in N:

$$\mathscr{L}_{2N}^{(0)}(u') = \mathscr{L}_N^{(\mathscr{I}_N)}(u') - \mathscr{N}; \qquad \mathscr{R}_{2N}^{(0)}(u') = \mathscr{R}_N^{(\mathscr{I}_N)}(u') + \mathscr{N}, \tag{24}$$

where $\mathscr{I}_N = \mathscr{I}(N, \varepsilon)$. $\mathscr{N}$ is a small constant, which we usually choose equal to a few grid spacings, to account for the possible fluctuations in the position of the minima $u_0(u')$ which can occur since the $G_N(u', u)$ are only discrete approximations to $G(u', u)$.

It is clear from Fig. 1b that one must be careful in applying (24). If a sufficiently high precision is obtained for a given grid M, where one of the $G_M(v, u)$, for fixed v, behaves as in Fig. 1b then the incorrect root u_1 will be bracketed as it corresponds to the minimum of $G_M(v, u)$. Upon doubling using (24), the root u_1 will remain bracketed and u_0, the correct minimum as $N \to \infty$, will be lost. Consider the effect that this will have on the discretized map $\tau_N(x)$. If v occurs in the limit cycle corresponding to the ground state then u_1 does as well by the definition of the map $\tau(u)$, and the wrong ground state will be obtained. If v does not occur in the ground state cycle then the wrong choice of minima will have no effect on the ground state though the effective potential will be incorrect.

One way to avoid the above problem is to scale the brackets $\mathscr{L}_N^{(k)}(u')$ and $\mathscr{R}_N^{(k)}(u')$ at some iteration $k = j$ before a precision is obtained that is sufficiently high to isolate the wrong minimum:

$$\mathscr{L}_{2N}^{(0)}(u') = \mathscr{L}_N^{(j)}(u') - \mathscr{N}; \qquad \mathscr{R}_{2N}^{(0)}(u') = \mathscr{R}_N^{(j)}(u') + \mathscr{N}. \tag{25}$$

This can be done by choosing j to be the first iteration which satisfies

$$\Delta_N^{(j)} < \phi(N). \tag{26}$$

The function $\phi(N)$ should be chosen to be larger than the largest possible intrinsic variation in $G_N(u', u)$ for u' and u. This is discussed more quantitatively in Section 3A.

The calculation time can be estimated for the case of both grid doubling and range restriction. When the brackets are scaled according to (25) then, for a given intermediate grid of M points, only a few of the possible values of u in $G_M^{(k)}(u', u)$ are bracketed for any given u'. On average there are $\eta^{(k)}$ such values, where $\eta^{(k)}$ is roughly equal to $2\mathscr{N}$ when k is small and tends towards 1.0 as $k \to \infty$. Only about $M\eta$ of the total βM^2 points are considered in one iteration of the algorithm to calculate $R_M(u)$, where η is a suitable average over k of $\eta^{(k)}$. A calculation similar to that leading to (11) and (12) gives

$$\begin{aligned} t_{ex} &= \eta t_p \left(\frac{N}{2^D}\right) \sum_{d=0}^{D} 2^d \mathscr{I}(N/2^{D-d}, \varepsilon_d) \\ &\approx \eta t_p N [\mathscr{I}_0 + \mathscr{I}_D] \end{aligned} \tag{27}$$

which is roughly linear in N whenever the $\mathcal{I}(N_l, \varepsilon_l)$ are not strongly N_l-dependent as is generally found to be the case numerically. The improvement in execution time of (27) over (12) is a factor of about $\beta N/\eta$ which, for a typical value of $\eta \approx 10$ and $\beta \approx 2$, should lead to calculations times roughly 200 times smaller for a typical grid of 1000 points. If the brackets are scaled according to (21), on the other hand, then $\eta^{(0)} = \beta N$ and the above value of η turns out to be roughly proportional to N. In this case the calculation time is given by a formula similar to (12) which is proportional to N^2.

E. *Site Elimination*

Site elimination is the name that is given to a further optimization that can be applied when range restriction is used and when the ground state, but not the effective potential, is sought. Consider the map $x = \tau_N(x')$, where we use x to denote one of the Q values of u that is part of the ground state sequence of grid points; Q is the period of the ground state configuration. It is easy to see that each x must be contained in the restricted region $\mathcal{S}_N^{(k)}(x')$. Define the new set of grid points in the following self-consistent way:

$$\mathcal{T}_N^{(k)} = \bigcup \mathcal{S}_N^{(k)}(u) \; \forall u \in \mathcal{T}_N^{(k)}.$$

$\mathcal{T}_N^{(k)}$ is the union of the sets $\mathcal{S}_N^{(k)}(u)$ for those values of u that are themselves in $\mathcal{T}_N^{(k)}$. The elements of the ground state, defined by the map $\tau_N(x)$, are trivially elements of $\mathcal{T}_N^{(k)}$ for all k. When k is sufficiently small, however, other grid points may also be contained in $\mathcal{T}_N^{(k)}$. The usefulness of $\mathcal{T}_N^{(k)}$ is that those u' that are not elements need not be considered in iterating (14). When k is large and $\mathcal{T}_N^{(k)}$ contains only a few elements, the resulting decrease in t_{ex} can be significant.

We implement site elimination only on the largest grid once the last grid doubling has been performed. For the few cases that we have examined in detail, it turns out that the improvement in the calculation time is roughly a factor of 2 or 3 in most cases with a slightly larger improvement occurring for configurations of large Q. Since most of the execution time is in the calculations at the largest grid size it was felt that including site elimination at grids other than the final grid would not lead to a large enough improvement in execution time to justify the extra program code. This has not been verified, however. Numerical results on the effect of site elimination on t_{ex} are presented in Section 3B.

3. Numerical Results

In this section we present numerical results: to provide a more quantative estimation of the errors present in the calculations, to justify certain assumptions that were made in Section 2, and finally to show the effects of the above-mentioned optimizations on the calculation time. The calculations were performed using Pascal on Definicon Systems coprocessor-cards DSI-020 and DSI-780 which run in

an IBM-PC environment [6]. The associated 68020 CPU and 68881 FPU provide roughly the same performance as that of a VAX 11/780. All of the data points that we consider are from different regions of the phase diagram for the model described in [7]. In this model the potentials in (1) are given by

$$V(x) = \frac{K}{\theta^2}\,[1 - \cos(x\theta)],$$

$$W(y) = -\tfrac{1}{2}(y-\gamma)^2 + \tfrac{1}{4}(y-\gamma)^4.$$

$V(x)$ is a substrate potential of depth $2K/\theta^2$ and period $2\pi/\theta$ and the interaction potential $W(y)$ has a double well form. Commensurate phases are described in terms of a three component *winding number* [7]:

$$\omega = P{:}Q{:}R,$$

where P, Q, and R are defined in [7]. In this work it is only necessary to know that Q is the number of atoms in one period of the ground state and we refer to it

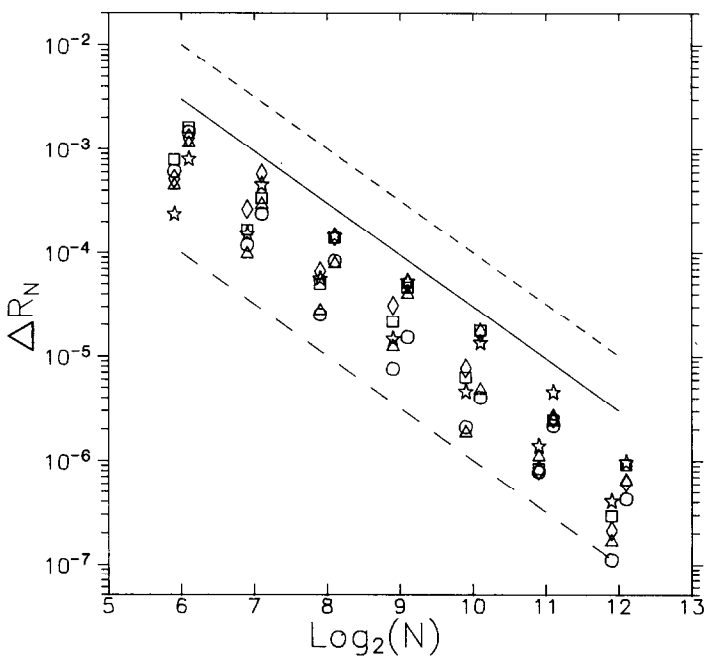

FIG. 2. ΔR_N^{rms} and $\Delta R_N^{\max}$ as functions of N. For clarity, points for ΔR_N^{rms} and $\Delta R_N^{\max}$ are displaced to the right and left, respectively. The points are calculated for points of different period: (○) $Q=1$; (□) $Q=2$; (△) $Q=5$; (◇) $Q=15$; (☆) $Q=26$. The solid line represents the upper bound for the intrinsic error given in (28). The long- and short-dashed lines are, respectively, the functions $\varepsilon(N)$ and $\phi(N)$ introduced in (9) and (26),

simply as the period of that phase. Our observations on a number of other models suggest that the numerical results presented here are typical.

A. *Intrinsic and Iteration Errors*

Values for ΔR_N^{rms} and $\Delta R_N^{\max}$ as a function of N are shown in Fig. 2 for ground states with period ranging from 1 to 26. The points for ΔR_N^{rms} are displaced slightly to the left of those for $\Delta R_N^{\max}$ for clarity. It is noteworthy that ΔR_N^{rms} and $\Delta R_N^{\max}$ only differ by about a factor of two indicating that R_N converges reasonably uniformly as $N \to \infty$. In addition, both fall into relatively narrow bands showing only a weak dependence on ω. These bands decay according to the power law $\Delta R_N \sim N^{-\alpha_{\text{int}}}$ with $\alpha_{\text{int}} \cong 1.66$. We assume that this power law is obeyed as $N \to \infty$ and we take the solid line in Fig. 2 as an upper bound for $\Delta R_N^{\max}$:

$$\Delta R_N^{\text{sup}} = A N^{-\alpha_{\text{int}}} \tag{28}$$

with $A = 3$. An upper bound for the intrinsic error of $R_N(u)$ for any u can be obtained by summing (28) over the appropriate N as N is doubled to ∞:

$$\mathscr{E}_{\text{int}}(N) \equiv |R_N(u) - R(u)| \lesssim \sum_{m=0}^{\infty} A(N2^m)^{-\alpha_{\text{int}}}$$

$$= \frac{1}{1 - 2^{-\alpha_{\text{int}}}} \Delta R_N^{\text{sup}} \cong 1.5\, \Delta R_N^{\text{sup}}.$$

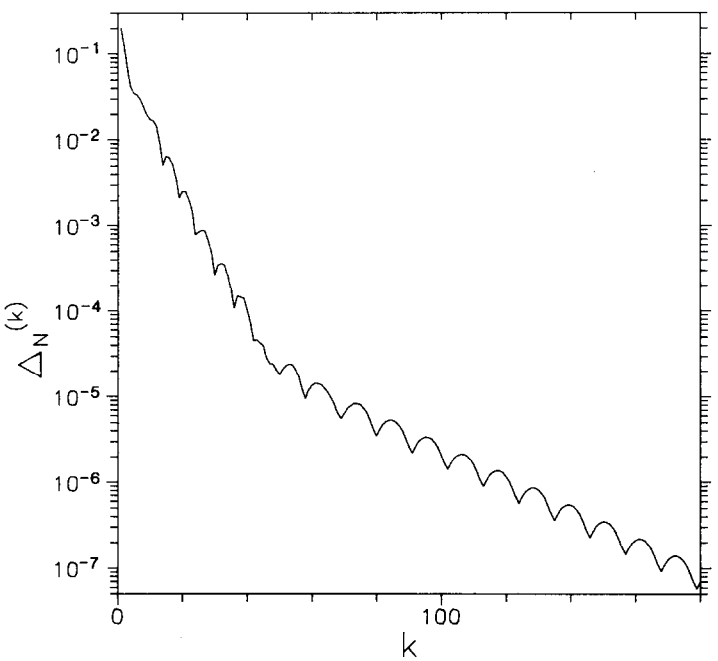

FIG. 3. $\Delta_N^{(k)}$ as a function of k for a phase of period $Q = 11$.

An analysis of the iteration error is not as straightforward as that of the intrinsic error. Figure 3 shows an example of the dependence of $\Delta_N^{(k)}$, defined in (8), on k. The data corresponds to a phase of period $Q = 11$ and for a grid of $N = 1024$ points. No grid doubling was performed. At large values of k ($\gtrsim 60$) the convergence is that of a modulated exponential with exponent $\alpha_Q = 0.042$ and with a modulation of period 11. Interestingly, this modulation period is always found to be equal to the periodicity, Q, of the eventual ground state. At smaller values of k ($10 \lesssim k \lesssim 40$) the convergence is similar but now with exponent $\alpha_q = 0.19$ and with a modulation period of between 5 and 6. It is worthy of note that, in the $K - \gamma - \theta$ phase diagram, this period 11 phase occurs in a region between two much larger regions where phases of period 5 and 6, respectively, are the groundstates. In fact, in going from the $Q = 5$ to the $Q = 6$ regions, a large number of higher period phases occur suggestive of a Devil's staircase like behavior (see [2, 7] for instance). Here we are only interested in the largest step corresponding to $Q = 11$. The numerical behavior is, in light of this observation, quite interesting and suggests that, initially for small k, convergence is toward the pure *undefected* phases with smallest period as suggested by the periodic modulation of $\Delta_N^{(k)}$ with period between 5 and 6. Only at higher values of k does the presence of higher order *defected* phases (smaller steps in the Devil's staircase) show up in the form of the convergence of $\Delta_N^{(k)}$. This interpretation is further supported by the observation that α_Q is found to have a definite

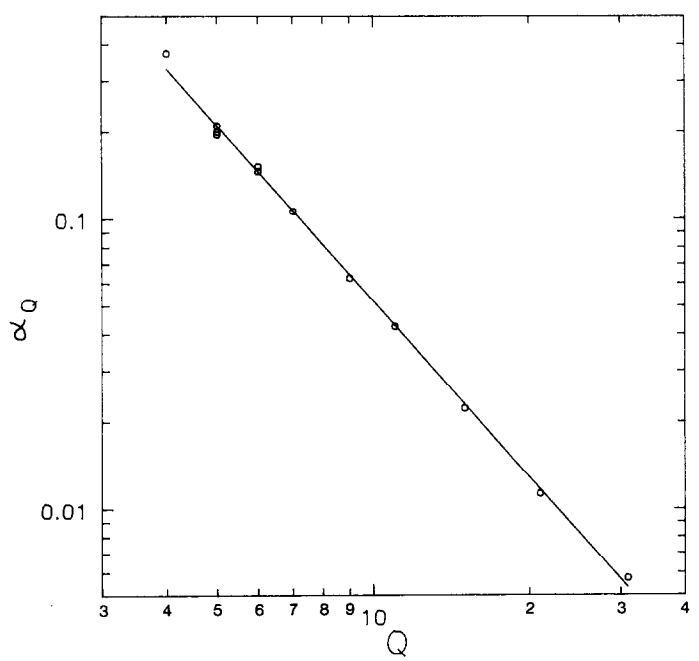

FIG. 4. α_Q as a function of Q for points from several different areas of the $K - \gamma - \theta$ parameter space.

dependence on Q as shown in Fig. 4. Phases from several widely separated regions of parameter space were used and it is found that, to within a few percent,

$$\alpha_Q = 5.4/Q^2. \tag{29}$$

This relation is well followed even by the intermediate exponential regions, when they occur, provided that the effective period q is used rather than Q (in the example in Fig. 3, $5 < q < 6$, for $10 \lesssim k \lesssim 40$).

This behavior of different periodically modulated exponential regions is typical of the cases that we have investigated. As one might expect, when regions of the phase diagram corresponding to even higher order steps in the Devil's staircase are considered then more exponential regions with different slope and different modulating periods can be identified.

Assuming the above periodically modulated exponentially decaying behavior to be typical then an estimate for the iteration error can be made. For $k \geqslant k_0$, for any given (positive) k_0, $\Delta_N^{(k)}$ is bounded from above by a function which can be written

$$\Delta^{ub}(k; k_0) = A(k_0)\, e^{-\alpha_Q (k - k_0)}. \tag{30}$$

An upper bound for the iteration error associated with $R_N^{(k_0)}$ is obtained by summing (30) from $k = k_0$ to $k = \infty$ which gives

$$\mathscr{E}_{it}(k_0) \equiv \max_u |R_N^{(k_0)}(u) - R_N^{(\infty)}(u)| \lesssim \frac{A(k_0)}{(1 - \exp(-\alpha_Q))}.$$

When α_Q is small ($Q^2 \gg 5.4$) then $\mathscr{E}_{it}(k_0) \approx A(k_0)/\alpha_Q \sim Q^2$.

From (20) and (29) one has that $g \lesssim Q^2/3$ (α_Q is equivalent to the α used in Section 2C). At a given point in parameter space the value that should be chosen for g depends on Q but knowledge of Q requires that the numerical method be applied with *some* value for g. In our numerical method we generally choose $g \approx 10$–20 which we find works fine in most cases, even when $Q \gg (3g)^{1/2}$. Occasionally this value for g is too small leading to wrong results. It is found that these wrong results tend to occur in a localized region of parameter space leading to areas of the phase diagram that do not agree with the expected behavior clearly indicating the presence of a problem.

Consider now the choice of $\varepsilon(N)$ that was introduced in Section 2A. In the grid doubling scheme, the precision $\varepsilon(N)$ should be chosen to have the same exponential dependence as ΔR_N. On one hand, $\varepsilon(N)$ should be chosen small so that R_N is a good approximation to R. On the other hand, because of the intrinsic error after

$\varepsilon(N)$ is chosen. A good choice is then to choose $\varepsilon(N)$ so that $\Delta_N^{(k)} \sim \varepsilon(N)$ when the intrinsic and iteration errors are roughly the same magnitude. This occurs when

$$\varepsilon(N) \cong \alpha_Q \frac{\mathscr{E}_{\text{int}}}{\alpha_{\text{int}}} \cong \frac{10}{Q^2}\, \mathscr{E}_{\text{int}}.$$

As with φ, the proper choice of $\varepsilon(N)$ requires prior knowledge of the final result. The $\varepsilon(N)$ that we have used and which is found to work well is shown by the long-dashed line in Fig. 2. An even simpler choice for $\varepsilon(N)$ that works well involves using one value, $\varepsilon_{d<D}$, for all but the final largest grid. For the largest grid a somewhat larger value ε_D is used. Good choices are $\varepsilon_{d<D} \cong \varepsilon(N/2)$ and $\varepsilon_D \cong \varepsilon(N)$. The threshold $\phi(N)$, introduced in Section 2D, should be chosen somewhat larger than $\Delta R_N^{\max}$ to avoid the problems described in Section 2D. The value that we use for the numerical results in Section 3B is shown by the short-dashed line in Fig. 2.

B. *Calculation Times for Different Levels of Optimization*

In this subsection we present numerical results for the time required to calculate $R(u)$ as a function of the grid size, N, and when different combinations of the optimizations, described in Section 2, are used. Figures 5 and 6 show the calculation times for one point as a function of the grid size N which, for convenience, we have taken to be a power of 2. In each case, several different combinations of optimization are considered. These are indicated in the legend in Fig. 5. In the four columns on the right of the legend, a letter represents the presence of a given

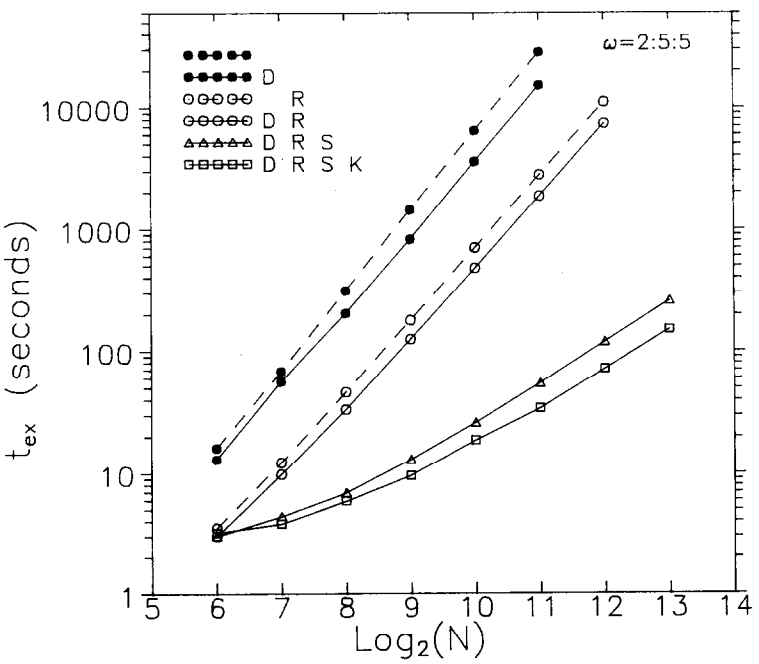

FIG. 5. Execution time for a point with period 5 as a function of N and for different levels of optimization. The presence/absence of one of D, R, S, or K in the legend indicates the presence/absence of the corresponding optimization: D = grid doubling; R = range restriction; S = boundary scaling using (25)—otherwise using (21); K = site elimination.

optimization whereas the absence of that letter means that that optimization was not used. The optimizations are:

D Grid doubling (Section 2B).

R Range restriction (Section 2C).

S Boundary scaling using (24); otherwise (21) is used.

K Site elimination (Section 2E).

For added clarity, solid/broken lines have been used to indicate the presence/absence of grid doubling. Similarly, open/solid symbols denote the presence/absence of range restriction. We denote the execution time by $t_{ex}[xy\cdots]$, where x, y, $\cdots$ are the symbols, described above, for the different optimizations that have been used. For instance, $t_{ex}[\ ]$ indicates that no optimizations are used, $t_{ex}[\mathrm{DR}]$ indicates grid doubling and range restriction and so on.

Consider Fig. 5 corresponding to a ground state with $Q = 5$. When no optimizations are present $t_{ex}[\ ]$ varies roughly as N^2 as expected by (10), since the number of iterations required for convergence is almost independent of N. With grid doubling it is found that $t_{ex}[\mathrm{D}]$ is roughly a factor of 2 smaller than $t_{ex}[\ ]$ with the same N^2 dependence. With range restriction only, a more significant improvement is noted and $t_{ex}[\mathrm{R}] \approx t_{ex}[\ ]/5$. With grid doubling and range restriction but

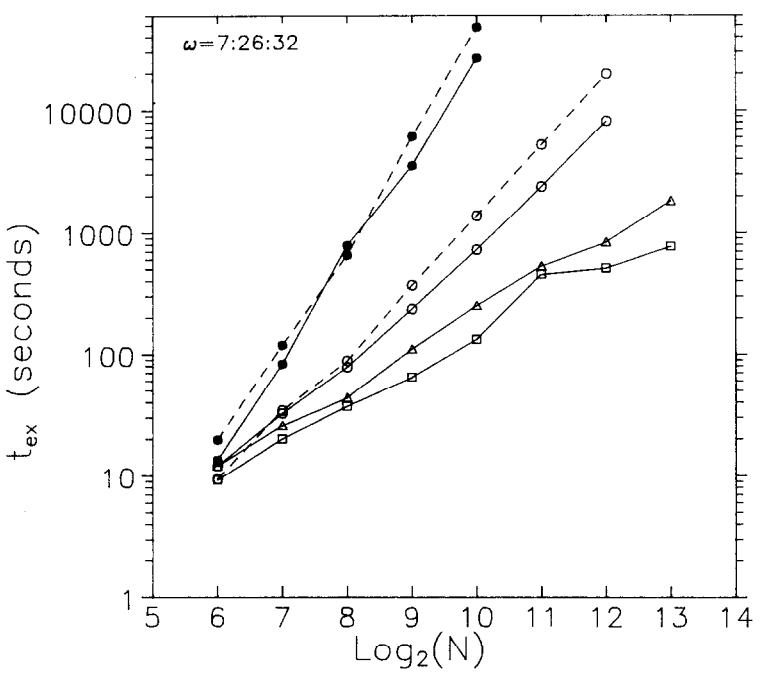

FIG. 6. Exacution time for a point with period 26 as described in the figure caption for Fig. 5.

with the bracketed regions scaled using (21) then $t_{ex}[\text{DR}] \approx t_{ex}[\ ]/10$. When the brackets are scaled using (25) one finds the biggest improvement in t_{ex} and, as expected from the disussion of Section 2D, $t_{ex}[\text{DRS}]$ varies roughly linearly with N. With site elimination, a small but significant improvement is noted. For large N, the total increase in speed is

$$t_{ex}[\ ]/t_{ex}[\text{DRSK}] \approx N/3.$$

We find the behavior shown in Fig. 5 for $Q = 5$ to be typical of the results when Q is relatively small. An example when Q is relatively large is shown in Fig. 6 for $Q = 26$. The behavior of the execution time as a function of N and the various optimizations is qualitatively the same as in Fig. 5 except for certain details. Both $t_{ex}[\ ]$ and $t_{ex}[\text{D}]$ increase somewhat faster that N^2. This occurs because the number of iterations required for convergence increases with N which in turn is a result of choosing $\varepsilon(N)$ to be a decreasing function of N.

Finally, we find the dependence of $t_{ex}[\text{DRSK}]$ with the ground state period Q to be roughly linear although there is a significant variation depending, for instance, on the exact region of the phase diagram being investigated and on the proximity of a given point in phase space to a phase boundary.

C. *Convergence of* $R_N^{(k)}(u)$ *with* $m = 0$

It was mentioned in Section 2A that $R_N^{(k)}(u)$ does not converge to $R_N(u)$ as $k \to \infty$ when $m = 0$ in (7). The behavior of $R_N^{(k)}(u)$ is, however, of some interest. Consider the symetric effective potential defined in (5). The discretized $F_N^{(k)}(u)$ is defined analogously to $R_N^{(k)}(u)$. At convergence, when $m = 1$, $F_N(u)$ has, for a ground state of period Q, Q minima of exactly the same depth. If (7) is iterated with $m = 0$ one finds instead that $\tilde{F}_N^{(k)}(u)$ converges to a cycle of period Q, where

$$\tilde{F}_N^{(k)}(u) = \tilde{F}_N^{(k+Q)}(u) + f_k$$

for each k, where $f_k \to 0$ as $k \to \infty$ (the tilde indicates calculation with $m = 0$). The actual rate of convergence to $\tilde{F}_N(u) \equiv \tilde{F}_N^{(\infty)}(u)$ is found to depend on Q in the same way as when $m = 1$. $\tilde{F}_N(u)$ shows the same inversion symmetry as does $F_N(u)$ and $R_N(u)$, though for a given k there are no longer Q equal minima. If, however, one calculates the average

$$\bar{F}_N(u) = \lim_{k \to \infty} \frac{1}{Q} \sum_{l=0}^{Q-1} \tilde{F}_N^{(k+l)}(u)$$

one finds, to within numerical precision, that $\bar{F}_N(u)$ has Q equivalent minima at the same positions as the Q minima of $F_N(u)$. The difference $F_N(u) - \bar{F}_N(u)$ is not zero to within numerical precision for finite N though it appears to converge to zero as

$N \to \infty$. The results of this section were found to occur in each of the few cases that were examined and, although the $m = 0$ case has not proved useful in improving our method of solving for the effective potentials, it may be of interest for future studies into solving equations such as (7).

4. Discussion

In this article we have presented a numerical method for solving for the discretized effective potentials and ground states for a certain class of problems involving classical one-dimensional chains of atoms with nearest neighbor interactions. The major advantage of our method is that the calculation time is found to vary roughly linearly with the size of the grid, N, on which the effective potential is discretized. This is to be compared with N^2 or worse when the optimizations are removed and with the difference between N^2 and N^3 when the modified Karp–von Golitchek algorithm [3] is used. The advantages of the latter method are that it finds the exact ground state and that it is easily vectorized as is the iterative method without optimizations or with just grid doubling. The optimized iterative scheme would not enjoy any large improvements in t_{ex} as a result of vectorization. Its much smaller execution time, however, means that, when implemented on a micro- or minicomputer, it is competitive with the other two methods being executed on systems, where vectorization is available. The main disadvantages of the optimized iterative method are the added complexity and the dependence on a larger number of numerically supported but not proven properties of the effective potentials. Verification by removing some of the optimizations to occasionally check the results as well as having a rough idea of how the results should behave is useful in applying the above methods. We have found that this method has permitted a detailed investigation into the phase diagrams of a number of different models with a modest amount of computing power.

It is worth discussing how the algorithm that we have presented might be extended to different models other that those described by (1). A generalization can be made, for instance, to include higher neighbor interaction terms. When up to second neighbor terms are included, (1) can be rewritten so as to have the same form but with u and u' replaced by two-component vectors $\mathbf{r}$ and $\mathbf{r}'$. The anisotropic next nearest neighbor Ising (ANNNI) model (see, for instance, [8]) and the elastic model of Janssen and Tjon [9] are two examples. In these cases $R_N(\mathbf{r})$ is defined on a square grid of N^2 points. Each grid doubling now increases the number of grid points by a factor of 4 and range restriction requires N^2 *pairs* of brackets. While the unoptimized algorithm would be expected to have $t_{ex} \sim N^4$, the optimized version should have $t_{ex} \sim N^2$ which is a considerable improvement. It should therefore be possible to obtain results on a grid of 100×100 points with about the same computational burden as that required for a grid of 10^4 points in the nearest neighbor case.

ACKNOWLEDGMENTS

The author thanks L. Floria and R. Griffiths for useful discussions concerning their numerical method and for making a preprint of their work available. The author also acknowledges the financial assistance of the Natural Sciences and Engineering Research Council (NSERC) of Canada and Fonds FCAR pour l'aide et le Soutien à la Recherche du Gouvernement du Québec.

REFERENCES

1. R. B. GRIFFITHS AND W. CHOU, *Phys. Rev. Lett.* **56**, 1929 (1986).
2. W. CHOU AND R. B. GRIFFITHS, *Phys. Rev. B* **34**, 6219 (1986).
3. L. M. FLORIA AND R. B. GRIFFITHS, Carnegie–Mellon University preprint (unpublished).
4. S. AUBRY, in *Structures et Instabilités* (les éditions e.p. de physique, Les Ulis Cedex (Paris), France), pp. 73–192.
5. R. CUNINGHAME–GREEN, *Minimax Algebra* (Springer-Verlag, New York, 1979).
6. see, for instance: BYTE, July 120 (1986) and August 108 (1986).
7. K. HOOD AND A. CAILLÉ, in preparation.
8. P. BAK AND J. VON BOEHM, *Phys. Rev. B* **21**, 5297 (1980).
9. T. JANSSEN AND J. A. TJON, *Phys. Rev. B* **25**, 3767 (1982).